MedChemComm

Accepted Manuscript

ROYAL SOCIETY OF CHEMISTRY

www.rsc.org/medchemcomm

MedChemComm

RSCPublishing

CONCISE ARTICLE

Synthesis and biological evaluation of potential small molecule inhibitors of Tumor Necrosis Factor

Cite this: DOI: 10.1039/x0xx00000x

Received 00th January 2012,
Accepted 00th January 2012

DOI: 10.1039/x0xx00000x

www.rsc.org/

Christos Papaneophytou[a,b], Polyxeni Alexiou[c], Athanasios Papakyriakou[d], Evangelos Ntougkos[e], Katerina Tsiliouka[f], Anna Maranti[f], Fotini Liepouri[f], Alexandros Strongilos[f], Anthi Mettou[a,b], Elias Couladouros[c], Elias Eliopoulos[d], Eleni Douni[d,e], George Kollias[e] and George Kontopidis[a,b*]

Inhibition of Tumor Necrosis Factor (TNF) production or function by small molecules has become a major focus in the pharmaceutical industry for the treatment of Rheumatoid Arthritis. In this study, a series of 39 novel SPD-304 analogs were designed, synthesized and evaluated as TNF inhibitors. Our results show that small structural changes produce ligands with similar binding affinities (K_d) for TNF, but significantly different potencies in a L929 cell-based assay. In addition, contrary to the high affinity of compounds **4e**, **8c** and **10e** for TNF *in vitro*, the potency of these compounds was determined to be low. We propose that these differences can partly be explained by the physicochemical characteristics of the synthesized SPD-304 analogs. Our findings were supplemented by molecular docking studies on the TNF dimer. These synthesized analogs may serve as a starting point for developing novel TNF inhibitors.

Introduction

Rheumatoid arthritis (RA) is a chronic disease characterized by synovial inflammation, as well as degeneration of cartilage and erosion of juxta-articular bone. RA affects about 0.5–1% of the general population causing increased morbidity and mortality mainly due to accelerated atherosclerosis.[1, 2] The inhibition of cytokines, particularly Tumor Necrosis Factor (TNF) that plays a pivotal role in regulating the inflammatory response in RA, has been successful in the treatment of RA.[3]

The synthetic therapeutic antibodies etanercept (Enbrel), infliximab (Remicade), and adalimumab Humira), bind to TNF directly, inhibiting the interaction between TNF and the tumor necrosis factor receptor (TNFR).[4] These agents have produced significant advances in RA treatment and validated the extracellular inhibition of this pro-inflammatory cytokine as an effective therapy.[5] The major disadvantages of these drugs are that they cannot be taken orally; they are expensive and could cause immunogenicity. This has stimulated the development of alternative small molecule-based therapies as inhibitors of TNF with improved efficacy, better tolerability, and oral administration.[5] An orally administered, small molecule that regulates TNF biology could either replace the injectable ones, or provide better disease control when used alone or in conjunction with existing therapies.[5] In addition, it is expected that rationally designed small molecule drugs based on scientific advancements and biotechnological improvements may reach, or even exceed the efficacy of protein drugs.[6] Thus, new therapeutic alternatives could be presented, with an improved outcome in the care of rheumatic patients.[6]

Up to the present time, only a small number of TNF inhibitors have been identified so far, and none of them have reached clinical trials.[7] Most of the small molecule inhibitors reported in the literature target TNF indirectly, by down-regulating the expression of TNF.[8-12] In 2010, Bandgar et al.[13] reported the synthesis and evaluation of a series of 2-hydroxy-β chlorovinyl-chalcones as inhibitors of TNF expression. In 2011, Wu et al.[14] reported the inhibition of TNF production from 6 chalcone derivatives, after screening 54 new synthetic chalcone compounds. In contrast, direct inhibition of TNF/TNFR interaction, by disrupting the active TNF trimer, has been an important strategy in the design and screening for small-molecule based TNF inhibitors.[15] However, only a few small molecules have been reported to directly disrupt TNF/TNFR interaction such as the polysulfonated naphthylurea, suramin and its analogs.[16] Furthermore the low potency and poor selectivity of suramin coupled with its tendency to cause adverse side effects renders it unsuitable for anti-TNF therapies.[17] In 2005, He et al.[18] reported a novel compound, SPD-304, which inhibited TNF activity by first promoting subunit disassembly of this trimeric cytokine and then binding to the resulting dimer. This mechanism was further confirmed by an X-ray structure of a single compound in complex with the TNF dimer. SPD-304 contains though the toxic 3-alkylindole moiety, which was found to be metabolized by cytochrome P450 enzymes through a dehydrogenation pathway similar to that of the potent pneumotoxin 3-methylindole, producing reactive electrophilic iminium species capable of reacting with protein and DNA targets.[19] In 2010, Chan et al.[20, 21] identified two small molecule TNF inhibitors, quinuclidine and quinolizine, from a natural product and natural-product-like chemical library using a structure-based virtual screening. Interestingly, quinolizidine was found to be more potent against TNF compared to SPD-304, while

quinuclidine displayed a comparable activity to SPD-304. Moreover, Kumar et al.[22] reported the synthesis of a series of iso-indolo [2,1-a]quinazoline derivatives as potent TNF inhibitors. In addition, the first metal-based direct inhibitor of TNF based on airidium (III) biquinoline complex has been reported.[23] Leung and co-workers[24] discovered two direct TNF inhibitors, Darifenacin (Enablex) and ezetimibe (Zetia), from a database of 3,000 US Food and Drug Administration (FDA)-approved drugs by applying structure-based virtual screening methods. Recently, Shen and co-workers[7] identified a new direct inhibitor of TNF with higher inhibition activity than SPD-304 in a cell based-assay, by performing a virtual screen on the SPECS database for molecules that TNF dimer structure.

To date, crystallographic structures of TNF with bound inhibitors have been reported only for SPD-304,[18] which is also one of the most active small molecule inhibitors. Therefore, SPD-304 is the more appropriate choice for structure-based design of TNF inhibitors. Recently, we have reported the synthesis of less toxic SPD-304 derivatives, by eliminating the 6′-methyl group of the 4-chromone moiety, and by incorporating electron- withdrawing substituents at the indole moiety.[25] In this study, we report the design and synthesis of 39 new SPD-304 analogs and their *in vitro* and cell-based evaluation against TNF provided valuable structure-activity relationships.

Results and discussion

Chemistry

Following our previous results[25], we have attempted to modify SPD-304 (Scheme 1) in 4 domains: i) modification of the chromone moiety (elimination of 6′-CH_3 or both methyl groups or substitution of the chromone moiety with other aromatic groups); ii) modification of the aromatic ring on the indole moiety; iii) conversion of the diamine to diamide; iv) coupling of the diamine bridge.

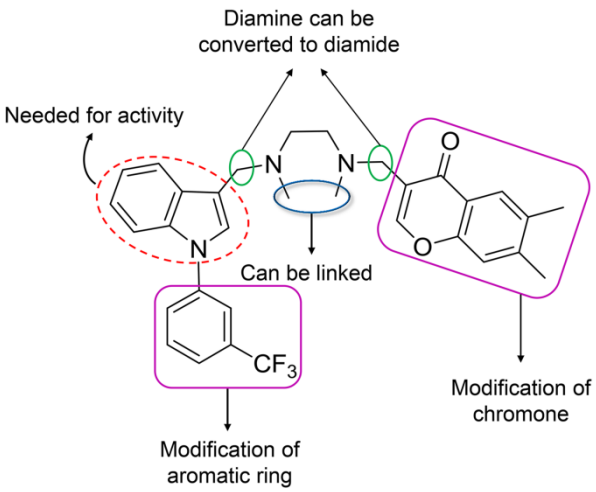

Scheme 1 Structural modifications of SPD-304

In this work, we describe the synthesis of 39 novel SPD-304 analogs that derived from the above mentioned modifications and are organized in 5 series (Tables 1-5).

Structure Activity Relationship Studies

The inhibitory effect of the synthesized compounds was initially examined in terms of their affinity for TNF by utilizing an *in vitro* fluorescence ligand-binding assay (Experimental Section).[26] Specifically, the change of fluorescence signal of three tyrosine residues located at the ligand-binding interface (Tyr59, Tyr119, Tyr151) is monitored upon titration of the ligands.[26] Fluorescence titration of TNF with the parent compound **1** (SPD-304; Fig. 1) yielded a K_d value of 5.36 ± 0.21 μM.[26] Titration of TNF with the SPD-304 analogs gave hyperbolic plots (Supporting Fig. S1), while Scatchard plot analysis gave linear plots indicating a single binding site (data not shown).

Our biological screening strategy was based on testing the capacity of the compounds to inhibit TNF functionality by employing the most widely used assay of TNF bioactivity.[27] The latter utilizes the ability of TNF to induce death in the murine fibrosarcoma cell line L929 following sensitization by the transcription inhibitor actinomycin D. If the compounds obstruct TNF activity at a functional level, they should prevent it from being cytotoxic in this setting. Initially, all compounds were tested using this assay at a concentration of 20 μM. Compounds showing at least a 25% inhibition of TNF-induced cell death were further tested to determine their IC_{50} values using the same assay in a dose-response way. It should be mentioned that as the basis of our screening is the protection from TNF-induced death, any compound that exhibited pronounced toxicity would not have passed our first line of testing. Having established that a selection of the compounds can obstruct TNF functioning, and given that TNF exerts its functions primarily through interacting with the TNF-R1[28] receptor, an ELISA-based test was devised to test their effects on this interaction.

A major problem experienced during this work was that a significant fraction of the tested compounds exhibited low aqueous solubility. This issue was overcome during binding affinity evaluation, by the addition of a co-solvent (either DMSO or PEG3350) in the reaction mixture, at a final concentration of 5%.[26] In addition, we employed a solubilisation protocol for this assay as previously described by our group.[26] It should be noted that TNF can tolerate both DMSO and PEG3350 up to 10% in the binding assay. However, those two co-solvents could not be used at this concentration in our cell-based assay, because they cause interference. As a result, many tested compounds may not have reached the desirable concentration for inhibition in this assay.

Fig. 1 summarizes the structures of the first series of compounds (**2a-2e, 3a-3d** and **4a-4f**) where we investigated the effect of the diamine cyclization of the lead compound **1**. Synthesis of these analogs was based on our previous docking studies.[25] The predicted conformation of these potential inhibitors, as derived from the docking studies, revealed that substitution by the more rigid piperazine ring results to a non-bound ligand conformation very similar to the bound one. Thus, compounds containing a coupled diamine bridge (transformation to piperazine) exhibit less variability with lower entropic cost due to the fixed conformation of the piperazine ring. Based on this observation, our initial point of modification was to reduce the binding energy of the parent compound **1** (SPD-304) by coupling the diamine bridge, leading to the compound **2a** and by elimination of 7′-CH_3 of the chromone moiety, without or with coupling of diamine bridge, in compounds **2b** and **2c** respectively (Fig. 1).

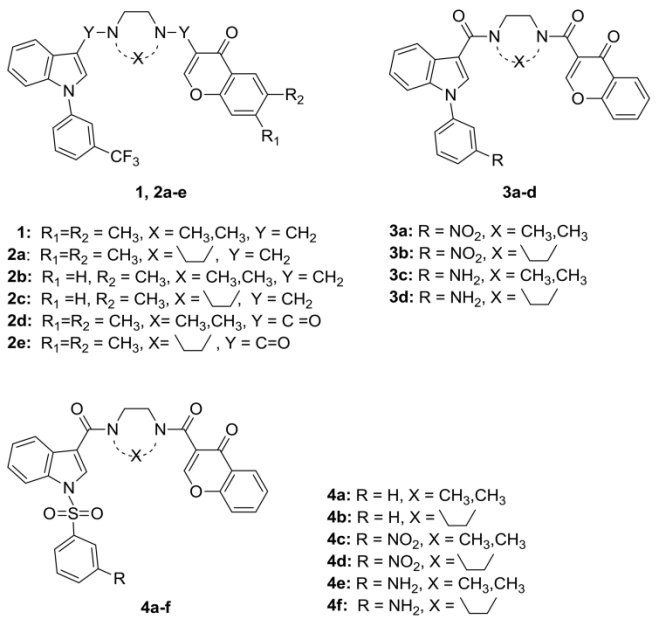

Fig. 1 Structures of SPD-304 derivatives **2a-e, 3a-d** and **4a-f**

The evaluation of the first series of compounds is presented in Table 1 where it can be seen that, although compounds **2a** and **2b** showed lower binding affinity compared to SPD-304, compound **2c** showed a K_d value close to that of SPD-304 (Table 1). Based on our previous results[25] we have also transformed the diamine parent compound to diamide analogs (**2d, 2e,** Fig. 1), with the aim to eliminate the toxic effect of the methylene group. Even though compound **2d**[25] exhibited approximately two-fold gain in affinity with respect to the parent compound **1**, it was approximately 5 times less potent. Compound **2e** displayed a comparable binding activity to SPD-304; however it was completely inactive in the cell-based assay (Table 1), probably due to its low solubility (data shown). It must be noted that assay conditions in binding determination, due to the presence of the organic solvent, allows the inhibitors to reach higher concentrations, thus the maximum inhibition could be observed.

Subsequently, the effect of variations of the substituents in the indole moiety of the parent compound **1** was investigated. Compounds **3a-3d and 4a-4f** (Fig. 1) were synthesized in order to explore the effect of different substitutions of *m*-trifluoromethylphenyl moiety of the carbonylated derivatives of lead compound **1,** in combination with demethylation of the chromone moiety. For each substituted compound the effect of the piperazine ring was also investigated. Initially, the trifluoromethyl group or the aromatic ring was substituted with either a nitro (**3a, 3b)** or an amino group (**3c, 3d**). In addition, the *m*-trifluoromethylphenyl moiety was substituted by the more electron-withdrawing phenylsulfonyl group in **4a**[25] and **4b** or with *m*-nitrophenylsulfonyl group in **4c** and **4d** or with an *m*-aminophenylsufonyl group in **4e** and **4f** (Fig. 1). Conversion of the diamine parent compound **1** to the diamide **3a-3d** and **4a-4f** and substitution of *m*-trifluoromethylphenyl with more electron withdrawing groups, led to a significant decrease of lipophilicity (Table 1). As outlined in Table 1, substitution of the trifluoromethyl group with either nitro (compounds **3a** and **3b**) or amino group (compounds **3c** and **3d**) resulted in a 2.5 to 7-fold decrease in binding affinity. Compounds **3a-3c** were completely inactive while compound **3d** revealed a two-fold loss in potency compare to initial lead **1**. Compounds **4a-4f** containing the *m*-substituent phenylsulfonyl group regained a fraction of the potency. Binding affinity results (K_d values) of **4a-4f** revealed that coupling of the diamine bridge had a negative impact. In addition, the K_d values of **4c-4g** indicate that the presence of an amino group promotes the binding affinity to TNF, while a nitro group is not a favorable substitution. Noticeably, the optimal binding affinity was shown by compound **4e** (K_d= 0.95 μM) which features a *m*-aminophenylsulfonyl group at the indole moiety (Table 1). We hypothesize that the markedly reduced activity of **4e** in the cell-based assay could be explained by its low bioavailability resulting from: i) poor cellular uptake and/or low solubility of this compound (data not shown) or ii) metabolic degradation of this compound. Overall, the affinity values of compounds **3b**, **3d**, **4b**, **4d** and **4f** suggest that introduction of the piperazine ring had a negative effect on their potency.

Table 1. Evaluation of the binding affinity and potency of the synthesized SPD-304 derivatives **2a-e**, **3a-d** and **4a-f**

ID	clogP[a]	TNF binding affinity[b] (K_d, μM)[c]	Inhibition of TNF activity[d] (IC_{50}, μM)[c]	Inhibition of TNF/TNFR1 interaction[e] (IC_{50}, μM)[c]
1[f]	8.0	5.36 ± 0.21	5.0 ± 1.5	5.0 ± 1.5
2a	7.9	10.12 ± 0.67	10 ± 1.9	15.0 ± 1.4
2b	7.5	18.64 ± 0.92	30 ± 2.2	10 ± 1.5
2c	7.4	4.78 ± 0.45	30 ± 3.1	15 ± 1.2
2d[f]	5.9	2.51 ± 0.16	20 ±0.6	>60
2e	5.7	5.12 ± 0.61	Inact	n.d
3a	3.9	12.22 ± 0.85	inact	n.d
3b	3.8	25.36 ± 1.25	Inact	n.d
3c	3.1	35.23 ± 1.92	Inact	n.d
3d	3.1	14.12 ± 0.69	10 ± 1.3	20 ± 1.8
4a[f]	3.3	7.00 ± 0.44	>60	>60
4b	3.6	12.81 ± 0.78	15 ± 1.7	40 ± 3.1
4c	3.1	3.16± 0.21	20 ± 1.6	40 ± 2.9
4d	3.0	16.82 ± 0.51	20 ± 2.1	40 ± 4.5
4e	2.5	0.95 ± 0.06	25 ± 1.8	20 ± 1.3
4f	2.4	5.45 ± 0.62	20 ± 1.9	40 ± 1.9

[a] Calculated using ChemDraw [b] Determination of binding affinity to TNF by fluorescence assay. [c] Mean ± SE (n=3 independents experiments); $p<0.05$. [d] Quantification of inhibition of TNF-induced death in L929 cells. [e] Quantification by TNF/TNFR1 ELISA. [f] data from[25]. "Inact"=inactive; "n.d."=not determined.

For the second series of compounds (**5a-5g** and **6a-6c**; Fig. 2) we substituted the chromone moiety with other aromatic groups, in order to investigate the effect of both shape and hydrophobicity on their binding affinity and potency. In compounds **5a-5g**, *m*-trifluoromethylphenyl has been replaced by the more electron-withdrawing phenylsulfonyl group (Fig. 2). The evaluation of the 2nd series of SPD-304 derivatives is summarized in Table 2. As it can be seen, replacement of the chromone moiety with naphthalene in the secondary and tertiary amines **5a** and **5b** resulted in a decrease of lipophilicity (cLogP 5.3 and 5.1, respectively). Introduction of the

naphthalene group resulted in a 7- and 5- fold decrease in the affinity of **5a** and **5b** with an increase in the K_d values compared to parent compound**.**

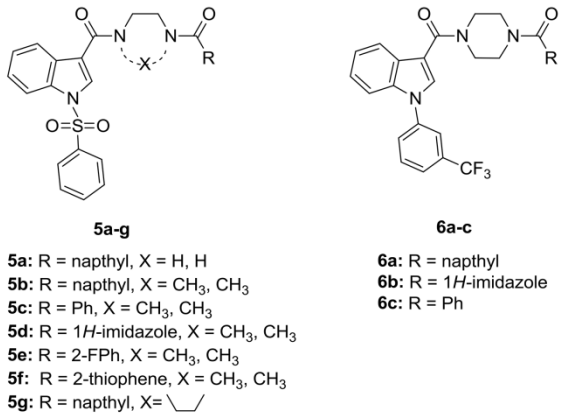

Fig. 2 Structures of SPD-304 derivatives **5a-g** and **6a-c**

Substitution of the chromone moiety with a phenyl group in **5c** (cLogP=5.0) had also a negative impact on its binding affinity. Substitution of the chromone moiety with 1*H*-imidazole and *o*-fluorobenzene in compounds **5d** and **5e** resulted in a significant reduction of their binding affinity. The presence of the smaller, but less hydrophobic, thiophene ring in **5f** led to a slight decrease (1.6-fold) in the binding affinity compared to **1**. Introduction of napthyl in **5g** resulted in a complete loss of binding affinity for TNF.

Table 2. Evaluation of the binding affinity and potency of the synthesized SPD-304 derivatives **5a-g**, and **6a-c**

ID	cLogP[a]	TNF binding affinity[b] (K_d, μM)[c]	Inhibition of TNF activity[d] (IC_{50}, μM)[c]	Inhibition of TNF/TNFR1 interaction [e] (IC_{50}, μM)[c]
5a	5.3	>35	Inact	n.d
5b	5.1	25.03 ± 1.88	inact	n.d
5c	5.0	17.27 ± 1.26	Inact	n.d
5d	2.8	Inact	Inact	n.d
5e	4.2	Inact	Inact	n.d
5f	3.1	8.22 ± 0.45	Inact	n.d
5g	3.9	Inact	inact	n.d
6a	6.8	Inact	Inact	n.d
6b	4.3	>35	Inact	n.d
6c	5.6	15.17 ± 1.34	Inact	n.d

[a] Calculated using ChemDraw. [b] Determination of binding affinity to TNF by fluorescence assay. [c] Mean ± SE (n=3 independent experiments); p<0.05. [d] Quantification of inhibition of TNF-induced death in L929 cells. [e] Quantification by TNF/TNFR1 ELISA. "Inact"=inactive; "n.d." =not determined.

To further explore the importance of the chromone moiety on binding affinity and potency, we kept the *m*-trifluoromethylphenyl moiety in the last three members of this series, with concurrent coupling of the diamide bridge (Fig. 2). Substitution of the chromone moiety with naphalene in **6a** and imidazole in **6b** resulted in complete loss of affinity for TNF. Finally, introduction of benzene in **6c** resulted in a 3-fold decrease in binding affinity (K_d=15.17 μM) with respect to the parent compound. Most notably, compounds **5a-g** and **6a-6c** lost their activity in the cell based-assay, indicating that the chromone moiety is essential to achieve TNF inhibition (Table 2).

Subsequently, the third series of compounds (**7a-7b**, **8a-8d** and **9a-9b**; Fig. 3) was designed in order to investigate whether the introduction of a nitro- or an amino- group at the 5′- position of the indole moiety could improve the ligands' binding affinity and potency for TNF.

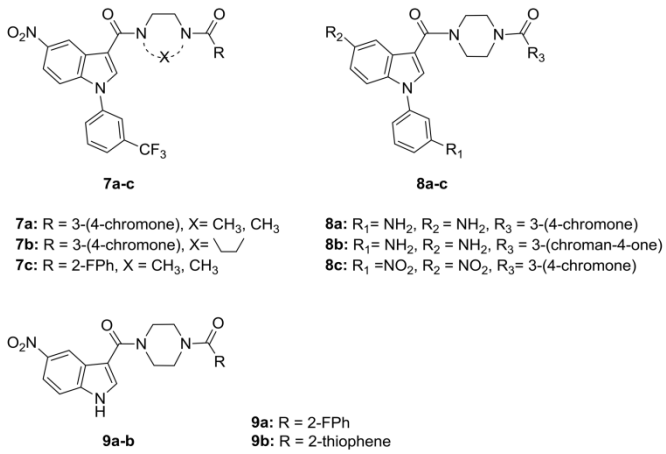

Fig. 3 Structures of SPD-304 derivatives **7a-c**, **8a-c** and **9a-b**.

In the first three members of this series (**7a-7c**), *m*-trifluoromethylphenyl remained intact, while the *H*-bond acceptor nitro group has been introduced in the 5′- position of the indole moiety.

Table 3. Evaluation of the binding affinity and potency of the synthesized SPD-304 derivatives **7a-c**, **8a-c** and **9a-b**

ID	cLogP[a]	TNF binding affinity[b] (K_d, μM)[c]	Inhibition of TNF activity[d] (IC_{50}, μM)[c]	Inhibition of TNF/TNFR1 interaction [e] (IC_{50}, μM)[c]
7a	4.8	13.28 ± 1.15	Inact	n.d
7b	4.8	Inact	Inact	n.d
7c	5.7	10.33 ± 1.16	Inact	n.d
8a	2.1	15.61 ± 1.46	40 ± 3.8	40 ± 3.1
8b	3.3	Inact	Inact	n.d
8c	3.6	0.74 ± 0.07	15 ± 1.4	20 ± 1.9
9a	2.5	17.85 ± 1.28	Inact	n.d
9b	2.0	10.74 ± 1.32	Inact	n.d

[a] Calculated using ChemDraw. [b] Determination of binding affinity to TNF by fluorescence assay. [c] Mean ± SE (n=3 independent experiments); p<0.05. [d] Quantification of inhibition of TNF-induced death in L929 cells. [e] Quantification by TNF/TNFR1 ELISA. "Inact"=inactive; "n.d." =not determined.

The results of **7a,** in which the chromone group has also remained intact, revealed a decrease in binding affinity,

compared to **1** (Table 3). Coupling of the diamine bridge in **7b** resulted in a complete loss of binding affinity, while replacement of the chromone moiety with *o*-fluorobenzene in **7c** displayed an increased K_d value (Table 3). Replacement of the *m*-trifluoromethylphenyl by *m*-aminobenzene and introduction of an amino group at the 5′ position of the indole ring in **8a** (the chromone moiety remained intact) and in **8b** (the chromone has been replaced by chroman-4-one) caused a significant decrease in both binding affinity and potency. Interestingly, substitution of the trifluoromethylene by the nitro group in **8c** resulted in a significant increase of affinity (K_d =0.74 μM) without any gain in potency, compared to SPD-304. This suggests that electron-withdrawing groups could enhance binding affinity, which is not directly linked to enhanced potency for TNF inhibition. Complete elimination of the *m*-trifluoromethylphenyl moiety in compounds **9a** and **9b,** in combination with substitution of the chromone moiety with *o*-flurobenzene and 2-thiophene, respectively, resulted in a predicted reduction of their lipophilicity (cLogP =2.5 and 2.0, respectively), followed by a large decrease of their binding affinity (Table 3). This supports our previous findings that larger substituents, such as chromone and naphthalene, are necessary to achieve significant inhibition.

In the fourth series of compounds (**10a**-**10e**; Fig. 4) we further investigated the importance of substitution in the 5′-position of the indole moiety. For this, derivatives containing or lacking a nitro group at this position were synthesized. In this series of compounds, the diamine bridge was cyclized to piperazine, and the amine conjugated to the chromone moiety of the initial lead was transformed to amide.

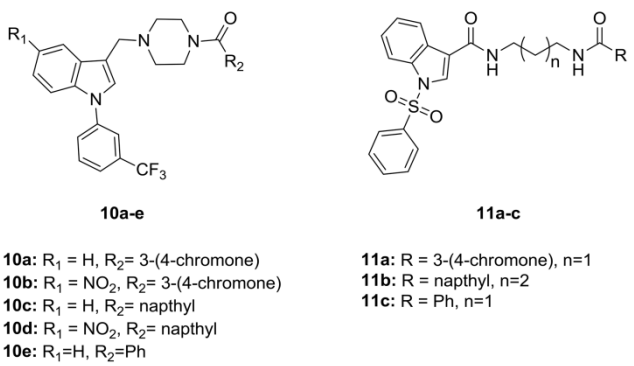

Fig. 4 Structures of SPD-304 derivatives **10a-e** and **11a-c**

Compound **10a** that lacks the 5′-nitro substituent showed a significant increase in binding affinity (K_d=1.6 μM), but a 2-fold decrease in potency compared to SPD-304 (Table 4). However, introduction of the electron-withdrawing nitro group in the 5′-position of the indole moiety in **10b** resulted in complete loss of potency. The influence of the 5′-substitution is also reflected on compounds **10c** and **10d,** in which the chromone moiety has been replaced by naphthalene. Specifically, compound **10c** lacking substitution in the 5′-position showed a 1.5-fold decrease in affinity and a 4-fold decrease in potency, while compound **10d** containing the 5′-nitro group was inactive. The latter supports the observation that both binding affinity and TNF activity can be altered dramatically by adjusting the electronic nature of the indole substituent. Interestingly, substitution of chromone by the smaller benzene ring in **10e** resulted in a 3-fold increase in binding affinity compared to **10c** that contains the naphthalene ring.

Table 4. Evaluation of the binding affinity and potency of the synthesized SPD-304 derivatives **10a-e**

ID	cLogP[a]	TNF binding affinity[b] (K_d, μM)[c]	Inhibition of TNF activity[d] (IC_{50}, μM)[c]	Inhibition of TNF/TNFR1 interaction [e] (IC_{50}, μM)[c]
10a	5.9	1.61 ± 0.15	10 ± 0.9	20 ± 2.2
10b	7.4	Inact	Inact	n.d
10c	7.7	7.82 ± 1.06	20 ± 1.8	40 ± 3.2
10d	7.5	Inact	Inact	n.d
10e	6.6	2.14 ± 0.16	15 ± 1.1	20 ± 1.7

[a] Calculated using ChemDraw. [b] Determination of binding affinity to TNF by fluorescence assay. [c] Mean ± SE (n=3 independent experiments); $p<0.05$. [d] Quantification of inhibition of TNF-induced death in L929 cells. [e] Quantification by TNF/TNFR1 ELISA. "Inact"=inactive; n.d. =not determined.

For the compounds of series 5 (**11a-11c**, Fig. 4), we have introduced three changes compared to SPD-304: i) the *m*-trifluoromethylphenyl substituent of the indole moiety was replaced by a phenylsulfonyl group, ii) the size of the diamine linker was modified, and iii) the chromone moiety was either maintained in **11a,** or was replaced by naphthalene in **11b** and benzene in **11c**. No change in binding affinity was observed when *m*-trifluoromethylphenyl was replaced by phenylsulfonyl group in **11a**, while this compound was significantly less potent than the lead compound **1**. However, compounds **11b** and **11c,** lacking the chromone moiety, were completely inactive. These examples further support the observation that activity can be significantly altered by changes in the size of the substituent.

Table 5. Evaluation of the binding affinity and potency of the synthesized SPD-304 derivatives **11a-c**

ID	cLogP[a]	TNF binding affinity[b] (K_d, μM)[b]	Inhibition of TNF activity[d] (IC_{50}, μM)[b]	Inhibition of TNF/TNFR1 interaction [d] (IC_{50}, μM)[b]
11a	4.6	5.2 ± 0.65	20 ± 1.9	40 ± 2.8
11b	5.4	18.75 ± 1.87	Inact	n.d
11c	4.3	Inact	Inact	n.d

[a] Calculated using ChemDraw. [b] Determination of binding affinity to TNF by fluorescence assay. [c] Mean ± SE (n=3 independent experiments); $p<0.05$. [d] Quantification of inhibition of TNF-induced death in L929 cells. [e] Quantification by TNF/TNFR1 ELISA. "Inact"=inactive; "n.d."=not determined.

Molecular Docking

In an effort to gain a better understanding of the structure-activity relationships of the synthesized compounds we employed *in silico* molecular docking calculations using the X-ray crystal structure of SPD-304 complex with a dimer of TNF subunits.[18] This structure revealed that the inhibitor binds in a shallow pocket within the subunit interfaces,

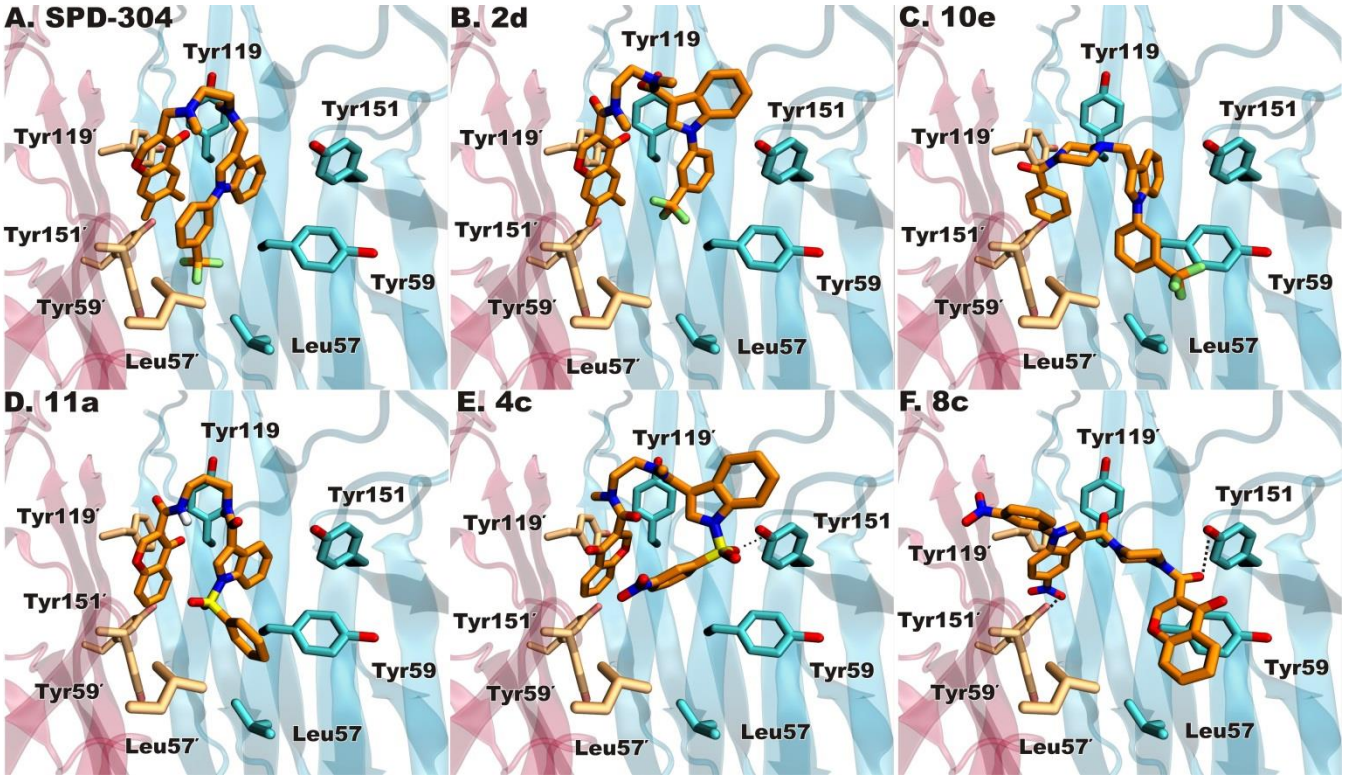

Fig. 5 Predicted conformations of the most active compounds in comparison with SPD-304 shown at exactly the same orientation. (A) The major interacting residues of the SPD-304 binding site that are colored with bright orange or cyan carbons for each TNF monomer, respectively. All other atoms are colored with blue for nitrogen, red for oxygen and green for fluorine. (C)–(F) Predicted conformations of the most active compounds **2d** (B), **10e** (C), **11a** (D), **4c** (E), and **8c** (F).

an interaction that is largely hydrophobic and shape-driven without any intermolecular hydrogen bonds or salt bridges.[18] The compound adopts a compact conformation, with the trifluoromethyphenyl indole and the dimethyl chromone moieties in a parallel arrangement, and the diamine linker exposed towards the bulk solvent (Fig. 5A and Fig. S2A of Supporting Information).

With the aim to provide structure-activity relationships between the synthesized analogs, we employed docking calculations at the ligand binding pocket of the TNF dimer, initially by performing re-docking of SPD-304. However, its crystallographic configuration proved to be highly problematic for molecular docking, exhibiting a large number of distinct conformational clusters with large deviations from the X-ray pose.[25] These results were considerably improved by using a more limited search space in combination with SMILES-generated initial coordinates for the inhibitor (see Experimental Section).

Docking of the synthesized analogs within the SPD-304 binding pocket revealed an equally high number of distinct conformational clusters, except for compounds bearing the more conformationally restricted piperazine linker. However, the top-ranked conformational clusters overestimated the binding affinity systematically (Supporting Table S1), as in the case of SPD-304. Considering that SPD-304 promotes disassembly of the TNF trimer mainly through a shape-driven interaction, we have also considered higher energy and less-populated conformational clusters that match the crystallographic pose of SPD-304 as much as possible. These conformations are designated as best-matched (Supporting Table S1) and exhibit a significantly better agreement between the estimated and the experimental dissociation constants of the most active analogs (i.e. $K_d^{exp} < 5.4$ μM). With a few exceptions, their interaction at the ligand-binding pocket of the TNF dimer is governed by hydrophobic and aromatic contacts, as in the case of SPD-304. A striking example is the best-matched conformation of **2d** (Fig. 5B) that displayed a two-fold improvement in the binding affinity with respect to the parent compound, and which could be attributed to the transformation of the diamine linker to the more rigid diamide analog. On the other hand, this modification imposes a change in the putative arrangement of the trifluoromethyphenyl indole and the dimethyl chromone moieties with respect to SPD-304, which is predicted to result in loss of interactions with the two Leu57 residues from each TNF monomer. In the same way, compounds **2e** and **2c**, which are even more conformationally restrained by the piperazine linker, display equipotent affinity with respect to SPD-304.

Examination of the predicted conformations that match the X-ray pose of SPD-304 reveal that either the dimethyl chromone in the case of **2e**, or the trifluoromethylphenyl ring in the case of **2c** might not be accommodated inside the ligand-binding pocket, which results in diminished interactions with Tyr151´ and Leu57/57´, respectively (Supporting Figs. S2B and S2C). It is thus possible that the expected energetic gain from the more rigid diamide and piperazine linkers is counterbalanced by a loss of hydrophobic interactions as a result of such conformational restriction. The significance of shape complementarity is demonstrated by

compound **10e** (K_d = 2.1 μM), which is the only potent inhibitor that lacks the chromone ring. In its place, the less bulky phenyl ring allows the ligand to be completely buried inside the pocket, albeit displaying fewer hydrophobic interactions (Fig. 5C). In contrast, the three-fold gain in the binding affinity of **10a** (K_d = 1.6 μM), that is not entirely buried inside the SPD-304 binding pocket, could be attributed to a potential hydrogen bond between the chromone keto group and the side chain of Tyr119 (Supporting Fig. S2D).

With the aim to increase the potential hydrogen bonding interactions of the synthesized analogs, we have introduced a sulfonyl group between the indole moiety and its phenyl substituent, which comprise polar nitro and amine groups as well. Among the potent inhibitors of TNF trimerization, compound **11a** is predicted to bind inside the binding pocket in a very similar configuration with respect to SPD-304 (Fig. 5D). Such a conformation may account for their equal binding affinities (~ 5 μM), since the polar amide and sulfonyl groups of **11a** are not engaged in any hydrogen bonding interactions. In contrast, the bulkier nitrobenzene ring of **4c** is predicted to force the indole moiety out of the binding pocket, so that a potential hydrogen bond might be formed between its sulfonyl group and the phenolic group of Tyr151 (Fig. 5E). Conversion of the 3-nitro group of **4c** to the corresponding amine in **4e** results in a 3-fold gain in binding affinity, which could be attributed to the better accommodation of the indole ring inside the binding pocket, in addition to the potential hydrogen bonding interaction between one of the two amide carbonyl groups of the linker and the side chain of Tyr119 (Supporting Fig. S2E). On the other hand, cyclization of the linker moiety to piperazine in the closely related analogue **4f** has a negative effect on the binding affinity, probably due to loss of hydrophobic interactions as in the case of **2e** (Supporting Fig. S2F). Finally, the lowest dissociation constant was displayed by the TNF inhibitor **8c** (K_d=0.74 μM) that comprises two nitro substituents on the phenyl indole moiety and a piperazine diamide linker, a combination that probably renders it too bulky to adopt the compact conformation of SPD-304 inside the binding pocket. Most importantly the experimental K_d value of 0.74 μM for compound **8c** is good in agreement with the predicted value of 0.32 μM (Supporting Table S1).As shown by the selected docked conformation of **8c** (Fig. 5F), its chromone ring could be stacked over the phenolic ring of Tyr59, while the 5-nitroindole moiety occupies the position of the dimethylchromone moiety of SPD-304. In such a configuration two potential hydrogen bonds with both Tyr151/151', in addition to the hydrophobic and aromatic interactions with Tyr119/119', Tyr59 and Leu57 may account for the high affinity of **8c** for the TNF dimer.

Although experimental data from X-ray crystallography are required to gain insight into more detailed structure-activity relationships of the synthesized compounds, our docking calculations suggest that a fine tuning of shape complementarity with the SPD-304 binding pocket and incorporation of polar groups at the appropriate positions could furnish more potent TNF inhibitors. More specifically, conversion of the diamine linker of SPD-304 to the corresponding diamide has a considerable contribution in the binding affinity of the analogs that combine a properly substituted phenylsulfonyl group on the indole moiety, such as **4e**. Similarly, incorporation of the more rigid piperazine linker may result in loss of the compact conformation as displayed by the X-ray structure of SPD-304, which could be compensated by additional polar groups that mediate hydrogen bonding interactions as in the case of **8c**. Considering that SPD-304 has been suggested to access the buried interior of the intact biologically active TNF trimer to form an intermediate complex that undergoes subunit dissociation, it is plausible that a number of the synthesized analogs are inactive inhibitors due to their inability to be properly accommodated at the interior of the TNF trimeric form, which further complicates the structure-based design process. In contrast, substitutions that result in bulkier ligands (that could not tolerate any adjustment in the binding pocket) will have such a profound effect on activity and report as inactive. K_d values higher than 40μM would be reported as inactive since that was the upper limit of the particular assay.

Conclusions

In this study we report the design, synthesis and biological evaluation of 39 novel SPD-304 analogs. Their binding affinity for TNF was determined using a fluorescence binding assay, and all compounds were also screened using a L929 cell-based assay at 20 μM concentration. Compounds that displayed at least 25% inhibition of TNF-induced cell death were subsequently tested using the same assay in a dose-response way to determine their IC_{50} values. Compounds **2a, 3b, 4b, 4c, 4d, 4f, 8c, 9a** and **9e** that exhibited IC_{50} values in the range of 10–20 μM were also tested in an ELISA-based assay. Taken together, the data from both assays indicated compound **2a** as having the most favorable profile with IC_{50}=10 μM in the L929 assay and IC_{50}=15 mM in the ELISA assay. To assist interpretation of our findings, a molecular docking study of this new class of ligands with TNF dimer was performed. Our results suggest that there is a correlation between shape complementarity of the strongest inhibitors within the SPD-304 binding pocked and their activity. Furthermore, substitution of *m*-trifluoromethylphenyl with the more electron- withdrawing *m*-amino-phenylsulfonyl (compound **4e**) or with *m*-nitrophenyl (compound **8c**) group at the indole moiety resulted in a considerable increase of their binding affinity. Therefore, incorporation of electron-withdrawing moieties can further improve the inhibitory activity of the SPD-304 derivatives.

Experimental

Chemistry

Unless otherwise stated, all reagents and solvents were obtained from commercial sources and used without further purification. Air sensitive chemistries were performed in dry and inert conditions under an atmosphere of argon. All reactions were routinely checked by TLC on Silica gel Merck 60 F_{254} and compounds were purified by column chromatography on silica gel using the appropriate solvent systems or by preparative HPLC. The purity of the tested compounds was determined by an analytical HPLC method and was found to be greater than or equal to 90% for all compounds unless otherwise stated. The purity analysis was performed on a HPLC Shimadzu 2010EV, equipped with a SPD-20A UV/Vis detector. Characterization of compounds was established by a combination of MS and NMR spectrometry techniques.^{1}H and ^{13}C NMR spectra were recorded on a Bruker Avance DRX spectrometer (500 MHz). Chemical shifts were presented in ppm (δ) with internal TMS standard. MS were obtained by the mass detector of the already mentioned HPLC Shimadzu 2010EV.

SPD-304 derivatives bearing the methylene moieties were prepared by reductive amination (route A, Scheme 2) of in the presence of a reducing agent. Different reported methods were

applied: A1) $NaBH(OAc)_3$/MeOH or/and DCE with or without pH adjustment with AcOH[29, 30], and A2) TMOF, $NaBH_3CN$.[31,32] The reductive amination reactions were complicated due to the likely formation of symmetrical byproducts from the reaction of aldehydes with diamines, as well as the extended reaction times and the difficulty in isolating and purifying the final products.

For the synthesis of the derivatives bearing the carbonyl groups the following typical amide coupling reactions (reaction B, Scheme 2) were applied: B1) N,N′-Carbonyldiimidazole-Mediated Amide Coupling in THF[33] and B2) Acyl-chloride formation from the corresponding acid with catalytic amount of DMF in THF (in certain cases the chloride was commercially available), followed by the coupling reaction in the presence of pyridine or thiethylamine in THF. [34, 35]

For the reduction of the nitro-substituent present in certain synthesized compounds the following methods were used depending on the substrate: C1) H_2, cat. Pd/C, EtOH/EtOAc, room temperature (rt), C2) $SnCl_2.2H_2O$, DMF, rt.[36]

Starting materials (substituted indole-3-aldehydes as well as 3-formyl-chromones) were synthesized according to reported procedures when not commercially available (data not included). It should be noted though that their acids were obtained by an oxidation reaction utilizing $NaClO_2$ / sulfamic acid in t-BuOH/H_2O and Jone's reagent in acetone respectively.[25]

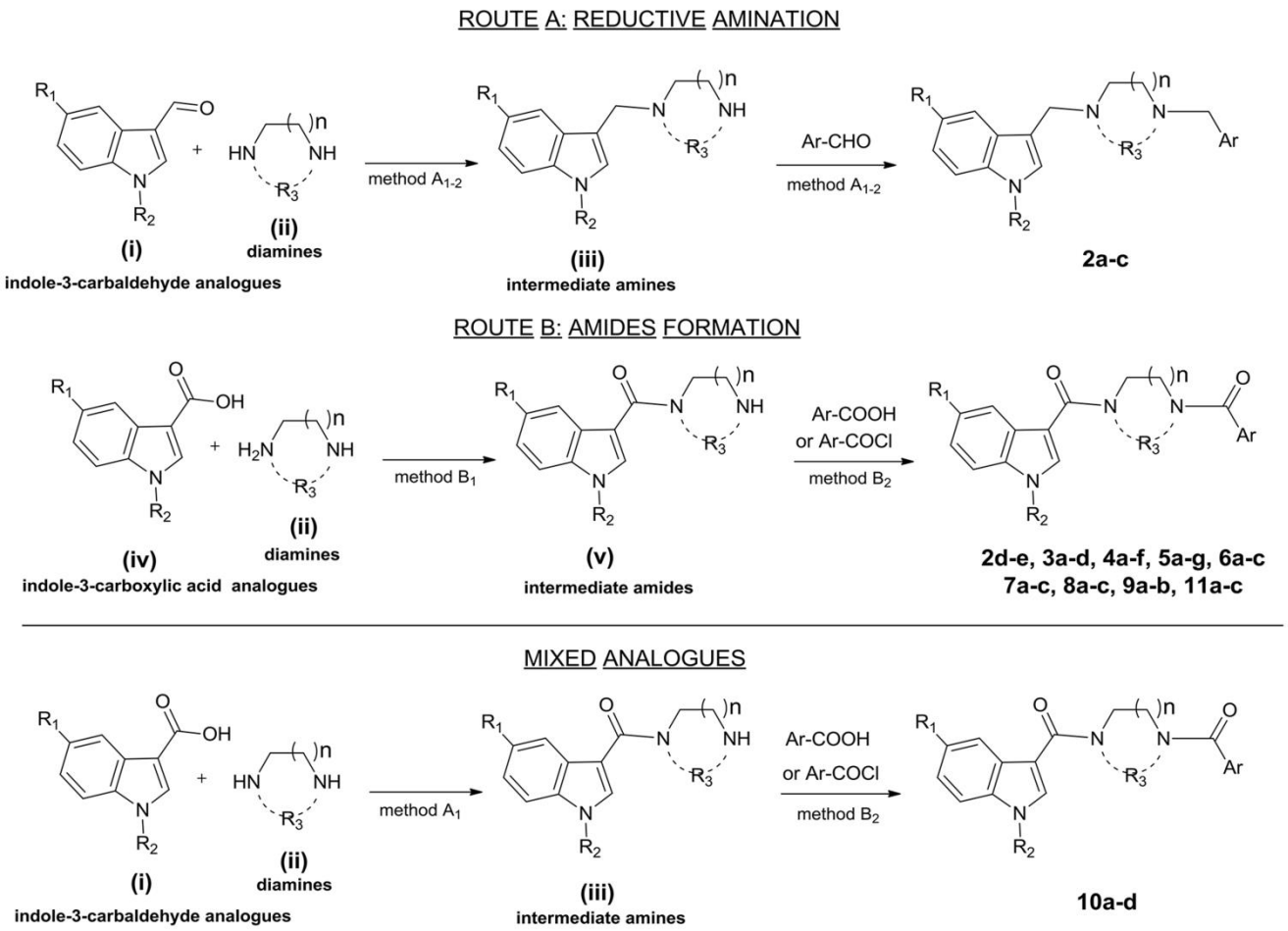

Scheme 2 General synthetic routes applied for the synthesis of key intermediates and target SPD-304 analogs

General procedures for the reductive amination reactions (Route A):

Method A1. Substituted indole-3-carbaldehyde (1 mmol) and access of the diamine **ii** (10 mmol) were mixed in MeOH (2.5 mL). The reaction pH was 6-7 and was carefully adjusted to pH=4-5 by addition of AcOH. The resulting mixture was stirred at rt for 24-48h and azeotropic removal of water was applied occasionally. MeOH was removed under reduced pressure and always under inert conditions, replaced with dichloroethane (2.5 mL) and treated with sodium triacetoxyborohydride (1.5 mmol). The reaction mixture was stirred until the limiting reactants were consumed or no further conversion was detected by TLC or IR. The solvent was concentrated in vacuo and the residue was purified by flash chromatography (gradient system: 2-10% MeOH/DCM) to provide the intermediate amines **iii**.

The latter intermediate amines **iii** (1 mmol) and the appropriate aromatic aldehyde (ex. 3-formyl-chromone) (1 mmol) were mixed in MeOH (2.5mL). Similar experimental procedure as above was applied and the target amine derivatives **2a** and **2c** were obtained.

2a. 6,7-dimethyl-3-((4-((1-(3-(trifluoromethyl)phenyl)-1H-indol-3-yl)methyl)piperazin-1-yl)methyl)-4H-chromen-4-one. Yield 40%. ^{1}H NMR (500 MHz, $CDCl_3$) δ= 7.95 (s, 1H), 7.80-7.78 (m, 2H), 7.73-7.71 (m, 1H), 7.68-7.61 (m, 2H), 7.55 (d, J=8.1Hz, 1H), 7.39-7.36 (m, 2H), 7.31-7.28 (m, 2H), 7.25-7.21 (m, 1H), 3.85 (s, 2H), 3.56 (s, 2H), 2.7 (br s, 8H), 2.40 (s, 3H), 2.37 (s, 3H); ESI-MS (m/z) calcd. for $C_{32}H_{31}F_3N_3O_2^+$ $[M+H]^+$ 546.24, found 546.01.

2c. 6-methyl-3-((4-((1-(3-(trifluoromethyl)phenyl)-1H-indol-3-yl)methyl)piperazin-1-yl)methyl)-4H-chromen-4-one (2c). Yield 24%, Purity 84%. ^{1}H NMR (500 MHz, $CDCl_3$) δ= 8.02 (s, 1H), 7.82-7.79 (m, 2H), 7.73-7.71 (m, 1H), 7.68-7.61 (m, 2H), 7.55 (d, J=7.84Hz, 1H), 7.48 (d, J=8.19Hz, 1H), 7.39-7.37 (m, 3H), 7.30-7.28 (m, 1H), 7.25-7.23 (m, 1H), 3.86 (s, 2H), 3.57 (s, 2H), 2.6 (br s, 8H), 2.47 (s, 3H) ; ESI-MS (m/z) calcd. for $C_{31}H_{29}F_3N_3O_2^+$ $[M+H]^+$ 532.22, found 532.00.

Method A2. To the substituted indole-3-carbaldehyde **i** (1 mmol) dissolved in trimethyl orthoformate (20 mL) under argon was added access of the diamine **ii** (2 mmol) and the solution was allowed to stir at room temperature for 5h. Sodium cyanoborohydride (1 mmol) was added and the solution was stirred for 24-48h. Water (0.5 mL) and MeOH (0.5 mL) were added and the solvent was then concentrated in vacuo. The residue was purified by flash chromatography (gradient system: 0-20% MeOH/DCM, followed by a mixture of 20% MeOH/DCM+5% NH_4OH) to provide the intermediate amines **iii**.

The latter intermediate amines **iii** (1 mmol) and the appropriate aromatic aldehyde (ex. 3-formyl-chromone) (1 mmol) were mixed in trimethyl orthoformate (20 mL). Similar experimental procedure as above was applied and the target amine derivative **2b** was obtained.

2b. 6-methyl-3-((methyl(2-(methyl((1-(3-trifluoromethyl) phenyl)-1H-indol-3-yl)methyl)amino)ethyl)amino)methyl)-4H-chromen-4-one. Yield 35 %. ^{1}H NMR (500 MHz, $CDCl_3$) δ= 8.02 (s, 1H), 7.79-7.65 (m, 7H), 7.53-7.51 (m, 2H), 7.41 (d, J=7.98 Hz, 1H), 7.04-6.98 (m, 2H), 4.61 (br s, 2H), 4.21 (br s, 2H), 3.47 (br s, 4H), 2.98 (s, 3H), 2.39 (s, 3H), 2.28 (s, 3H); ESI-MS (m/z) calcd. for $C_{31}H_{31}F_3N_3O_2^+$ $[M+H]^+$ 534.24, found 533.75 .

General Procedures for the amide coupling reactions (Route B):

Method B1. A mixture of substituted indole-3-carboxylic acid analogs **iv** (1 mmol) and N,N'-carbonyldiimidazole (CDI) (1.1 mmol) were dissolved in dry THF (12 mL) and stirred for 3-5h and at that time access of the diamine **ii** (10 mmol) was added at one portion. The reaction was left under stirring at room temperature for 20-24h, the volatiles were removed under reduced pressure and the residue was subjected to purification with flash chromatography (gradient system: 0-30% MeOH/DCM) to provide the intermediate amides **v**.

Method B2. To a solution of chromone-3-carboxylic acid or other appropriate carboxylic acid analogue (1 mmol) in dry THF (10 mL) was added an excess of oxalyl chloride (10 mmol), followed by DMF (0. 1 mL). The resulting mixture was stirred at room temperature for 1h and at that time the solvent was evaporated in vacuum and co-evaporated three times. The residue was dried under high vacuum for 10 min giving the respective acid chloride as a solid. In certain cases the acid chlorides used were commercially available.

The previously synthesized acid chloride or commercially available one (1 mmol) was dissolved in THF (10 mL) and pyridine (3.55 mmol) as well as the intermediate amides **v** (1 mmol) were added. The mixture was stirred for 20-24h and removal of the solvent gave a viscous residue, which was dissolved in ether (20 mL) and washed with saturated $NaHCO_3$ (2x10 mL) , water (1×10 mL), 1N HCl (2x10 mL), water (1×10 mL) and brine (1× 10mL). The organic portions were combined and dried over Na_2SO_4. Removal of the solvents produced a residue, which was subjected to flash chromatography (gradient system: 0-10% MeOH/DCM) to provide the target amide derivatives **2e, 3a-b, 4b-d, 5a-g, 6a-c, 7a-c, 8c, 9a-b** and **11a-c**.

2e. 6,7-dimethyl-3-(4-(1-(3-(trifluoromethyl)phenyl)-1H-indole-3-carbonyl)piperazine-1-carbonyl)-4H-chromen-4-one. Yield 77%. ^{1}H NMR (500 MHz, $CDCl_3$) δ=8.16 (s, 1H), 7.94 (s, 1H), 7.79 (s, 1H), 7.78 – 7.74 (m, 1H), 7.76 – 7.64 (m, 3H), 7.49 (d, J = 5.0 Hz, 1H), 7.31 (d, J = 7.3 Hz, 3H), 7.17 (d, J = 6.8 Hz, 1H), 3.90 (s, 4H), 3.86 (s, 2H), 3.43 (s, 2H), 2.40 (s, 3H), 2.36 (s,3H); ^{13}C NMR (125.5 MHz, $CDCl_3$) δ 173.97, 166.54, 163.73, 157.03, 154.75, 145.40, 139.26, 135.77, 130.75, 130.17, 127.94, 126.56, 125.75, 124.34, 124.07, 122.53, 122.05, 121.61, 120.88, 118.46, 112.99, 110.86, 47.78, 42.84, 20.56, 19.46; ESI-MS (m/z) calcd. for $C_{32}H_{27}F_3N_3O_4^+$ $[M+H]^+$ 573.19, found 573.63.

3a. N-methyl-N-(2-(N-methyl-4-oxo-4H-chromene-3-carboxamido)ethyl)-1-(3-nitrophenyl)-1H-indole-3-carboxamide. Yield 92%. ^{1}H NMR (500 MHz, $CDCl_3$) δ= 8.47 (s, 1H), 8.22 (dd, J = 26.1, 7.8 Hz, 2H), 8.01 – 7.82 (m, 3H), 7.79 – 7.59 (m, 3H), 7.53 (t, J = 8.1 Hz, 1H), 7.44 (dd, J = 15.6, 8.0 Hz, 2H), 7.32 (d, J = 3.6 Hz, 2H), 4.02 – 3.74 (m, 4H), 3.38 (s, 3H), 3.08 (s, 3H); ^{13}C NMR (125.5 MHz, $CDCl_3$) δ 173.73, 167.19, 165.26, 156.10, 149.15, 139.98, 135.45, 134.29, 130.96, 130.80, 130.18, 129.09, 126.02, 125.87, 124.26, 124.18, 124.08, 122.55, 122.47, 121.91, 121.80, 121.74, 119.32, 119.20, 118.35, 118.28, 110.27, 37.23, 33.57; ESI-MS (m/z) calcd. for $C_{29}H_{25}N_4O_6^+$ $[M+H]^+$ 524.17, found 524.36.

3b. 3-(4-(1-(3-nitrophenyl)-1H-indole-3-carbonyl)piperazine-1-carbonyl)-4H-chromen-4-one. Yield 52%. ^{1}H NMR (500 MHz, $CDCl_3$) δ= 8.42 (s, 1H), 8.29 (d, J = 8.0 Hz, 1H), 8.23 (s, 1H), 7.88 (d, J = 7.5 Hz, 1H), 7.80-7.68 (m, 4H), 7.52 (t, J = 8.3 Hz, 2H), 7.47 (t, J = 7.3 Hz, 2H), 7.37 – 7.31 (m, 2H), 3.91 (s, 8H); ^{13}C NMR (125.5 MHz, $CDCl_3$) δ 173.97, 165.94, 163.21, 157.26, 156.18, 149.29, 139.92, 135.61, 134.54, 131.04, 130.23, 129.55, 126.87, 126.29, 126.17, 124.35, 122.75, 122.60, 122.08, 121.13, 119.46, 118.42, 114.07, 110.70, 47.75, 42.80; ESI-MS (m/z) calcd. for $C_{29}H_{23}N_4O_6^+$ [M+H]+ 523.16, found 522.75.

4b. 3-(4-(1-(phenylsulfonyl)-1H-indole-3-carbonyl)piperazine-1-carbonyl)-4H-chromen-4-one. Yield 67%. ^{1}H NMR (500 MHz, $CDCl_3$) δ= 8.21 (s, 2H), 7.98 (d, J = 8.3 Hz, 1H), 7.91 (d, J = 7.8 Hz, 2H), 7.79 (s, 1H), 7.72 (t, J = 7.7 Hz, 1H), 7.62 (d, J = 7.9 Hz, 1H), 7.56 (t, J = 7.4 Hz, 1H), 7.52 – 7.41 (m, 4H), 7.36 (t, J = 7.7 Hz, 1H), 7.29 (t, J = 7.5 Hz, 1H), 3.80 (s, 6H), 3.39 (s, 2H) ; ESI-MS (m/z) calcd. for $C_{29}H_{24}N_3O_6S^+$ $[M+H]^+$ 542.14, found 541.65.

4c. N-methyl-N-(2-(N-methyl-4-oxo-4H-chromene-3-carboxamido)ethyl)-1-(3-nitrophenylsulfonyl)-1H-indole-3-carboxamide. Yield 35%. ^{1}H NMR (500 MHz, $CDCl_3$) δ = 8.32 (s, 1H), 7.90 – 7.60 (m, 3H), 7.59 (m, 1H), 7.54 (d, J = 8.3 Hz, 1H), 7.38 – 7.03 (m, 3H), 7.01 – 6.86 (m, 3H), 6.84 (s, 1H), 6.77 (s, 1H), 4.41 (br s, 4H), 2.79 (s, 3H), 2.56 (s, 3H); ^{13}C NMR (125.5 MHz, $CDCl_3$) δ 173.85, 165.63, 165.40, 156.18, 155.88, 148.35, 139.78, 134.49, 134.40, 132.46, 131.27, 131.13, 129.06, 128.81, 128.64, 126.72, 126.18, 126.14, 126.10, 124.84, 124.36, 122.36, 121.95, 118.48, 118.38, 113.37, 45.34, 38.51, 37.37; ESI-MS (m/z) calcd. for $C_{29}H_{25}N_4O_8S^+$ $[M+H]^+$ 589.14, found 588.79.

4d. 3-(4-(1-(3-nitrophenylsulfonyl)-1H-indole-3-carbonyl) piperazine-1-carbonyl)-4H-chromen-4-one. Yield 94%.^{1}H NMR (500 MHz, $CDCl_3$) δ = 8.27 (s, 1H), 7.92 (d, J = 8.0 Hz, 1H), 7.78 –

7.65 (m, 3H), 7.52 (d, J = 8.1 Hz, 1H), 7.29 (s, 1H), 7.26 – 7.15 (m, 2H), 7.16 (d, J = 7.8 Hz, 1H), 7.05 – 6.89 (m, 3H), 6.86 (t, J = 7.4 Hz, 1H), 3.33 (s, 4H), 2.97 – 2.82 (m, 4H); ^{13}C NMR (125.5 MHz, $CDCl_3$) δ 174.00, 163.98, 163.23, 162.14, 157.42, 156.18, 148.47, 139.72, 134.59, 134.39, 132.35, 131.26, 128.86, 128.55, 126.40, 126.30, 126.22, 126.07, 124.99, 124.34, 122.45, 122.37, 121.45, 118.43, 118.25, 113.51, 47.60, 42.64; ESI-MS (m/z) calcd. for $C_{29}H_{23}N_4O_8S^+$ $[M+H]^+$ 587.12, found 586.65 .

5a. N-(2-(2-naphthamido)ethyl)-1-(phenylsulfonyl)-1H-indole-3-carboxamide. Yield 20%. ^{1}H NMR (500 MHz, $CDCl_3$) δ= 8.38 (s, 1H), 8.11 (s, 1H), 8.08 (d, J = 7.9 Hz, 2H), 7.99 – 7.91 (m, 2H), 7.91 – 7.85 (m, 4H), 7.60 – 7.46 (m, 3H), 7.39 – 7.28 (m, 3H), 6.99 (s, 1H), 3.80 (s, 4H), 3.66 (s, 2H) ; ESI-MS (m/z) calcd. for $C_{28}H_{24}N_3O_4S^+$ $[M+H]^+$ 498.15, found 497.65.

5b. N-methyl-N-(2-(N-methyl-2-naphthamido)ethyl)-1-(phenylsulfonyl)-1H-indole-3-carboxamide. Yield 49%. ^{1}H NMR (500 MHz, $CDCl_3$) δ= 7.99 (d, J = 8.2 Hz, 1H), 7.92 (d, J = 8.6 Hz, 3H), 7.88 (d, J = 6.3 Hz, 3H), 7.79 (s, 1H), 7.64 (d, J = 7.8 Hz, 1H), 7.56 (dd, J = 10.4, 6.5 Hz, 3H), 7.48 (dd, J = 14.6, 7.4 Hz, 3H), 7.38 (t, J = 7.7 Hz, 1H), 7.31 (t, J = 7.4 Hz, 1H), 3.74 (br s, 10H); ESI-MS (m/z) calcd. for $C_{30}H_{28}N_3O_4S^+$ $[M+H]^+$ 526.18, found 525.75 .

5c. N-methyl-N-(2-(N-methylbenzamido)ethyl)-1-(phenylsulfonyl)-1H-indole-3-carboxamide. Yield 39%. ^{1}H NMR (500 MHz, $CDCl_3$) δ= 7.98 (d, J = 8.2 Hz, 1H), 7.93 – 7.69 (m, 4H), 7.53 (t, J = 8.7 Hz, 1H), 7.42 – 7.29 (m, 9H), 3.90 (br s, 3H), 3.34 – 3.17 (m, 4H), 3.06 (br s, 3H); ESI-MS (m/z) calcd. for $C_{26}H_{26}N_3O_4S^+$ $[M+H]^+$ 476.16, found 475.79.

5d. N-methyl-N-(2-(N-methyl-1H-imidazole-1-carboxamido) ethyl)-1-(phenylsulfonyl)-1H-indole-3-carboxamide. Yield 75%. ^{1}H NMR (500 MHz, $CDCl_3$) δ= 7.99 (d, J = 8.4 Hz, 1H), 7.86 (d, J = 7.1 Hz, 2H), 7.66 (t, J = 8.2 Hz, 2H), 7.60 (d, J = 8.1 Hz, 1H), 7.55 – 7.49 (m, 2H), 7.47 (s, 1H), 7.42 – 7.34 (m, 2H), 7.31 (d, J = 7.7 Hz, 2H), 3.94 (br s, 3H), 3.65 (br s, 2H), 3.24 (s, 3H), 3.20 (s, 2H); ESI-MS (m/z) calcd. for $C_{23}H_{24}N_5O_4S^+$ $[M+H]^+$ 466.15, found 465.79.

5e. N-(2-(2-fluoro-N-methylbenzamido)ethyl)-N-methyl-1-(phenylsulfonyl)-1H-indole-3-carboxamide. Yield 45%. ^{1}H NMR (500 MHz, $CDCl_3$) δ = 7.98 (d, J=8.10Hz, 1H), 7.88 (d, J=6.81Hz, 2H), 7.81-7.78 (m, 1H), 7.75-7.72 (m, 1H), 7.55-7.51 (m, 1H), 7.43-7.30 (m, 4H), 7.28-7.20 (m, 2H), 7.12-7.02 (m, 2H), 3.88 (br s, 3H), 3.51 (br s, 1H), 3.24 (s, 3H), 2.97 (s, 2H), 2.87 (s, 1H) ; ESI-MS (m/z) calcd. for $C_{26}H_{25}FN_3O_4S^+$ $[M+H]^+$ 494.15, found 493.75.

5f. N-methyl-N-(2-(N-methylthiophene-2-carboxamido)ethyl)-1-(phenylsulfonyl)-1H-indole-3-carboxamide. Yield 58%. ^{1}H NMR (500 MHz, $CDCl_3$) δ= 7.94 (d, J=7.85Hz, 1H), 7.86-7.83 (m, 2H), 7.69-7.67 (m, 1H), 7.62 (d, J=7.03Hz, 1H), 7.52 (d, J=6.59Hz, 1H), 7.43-7.40 (m, 3H), 7.35-7.29 (m, 2H), 7.23 (d, J=8.49Hz, 1H), 6.98 (br s, 1H), 3.87 (br s, 3H), 3.35 (br s, 4H), 3.17 (br s, 3H); ESI-MS (m/z) calcd. for $C_{24}H_{24}N_3O_4S_2^+$ $[M+H]^+$ 482.12, found 481.78.

5g. (4-(2-naphthoyl)piperazin-1-yl)(1-(phenylsulfonyl)-1H-indol-3-yl)methanone (5g), Yield 62%. ^{1}H NMR (500 MHz, $CDCl_3$) δ= 7.99 (d, J = 8.1 Hz, 1H), 7.94-7.91 (m, 3H), 7.89-7.85 (m, 3H), 7.80 (s, 1H), 7.64 (d, J = 7.8 Hz, 1H), 7.59-7.52 (m, 3H), 7.47 (q, J = 17.4, 9.3 Hz, 3H), 7.37 (t, J = 7.6 Hz, 1H), 7.30 (t, J = 7.4 Hz, 1H), 3.73 (br s, 8H); ^{13}C NMR (125.5 MHz, $CDCl_3$) δ 170.93, 164.68, 137.92, 134.62, 134.07, 132.89, 132.52, 129.77, 128.78, 128.65, 128.43, 128.06, 127.58, 127.39, 127.20, 127.13, 126.79, 125.91, 124.47, 124.31, 121.15, 116.87, 113.82, 66.04, 29.90, 15.48; ESI-MS (m/z) calcd. for $C_{30}H_{26}N_3O_4S^+$ $[M+H]^+$ 524.16, found 523.76.

6a. (4-(2-naphthoyl)piperazin-1-yl)(1-(3-(trifluoromethyl)phenyl)-1H-indol-3-yl)methanone. Yield 88% ^{1}H NMR (500 MHz, $CDCl_3$) δ= 7.96 – 7.84 (m, 5H), 7.82 – 7.71 (m, 2H), 7.69 (d, J = 8.0 Hz, 2H), 7.63 (d, J=6.98, 1H), 7.59 – 7.46 (m, 5H), 7.33 – 7.29 (m, 1H), 3.83 (br s, 8H); ESI-MS (m/z) calcd. for C31H25F3N3O2+ [M+H]+ 528.19, found 527.75.

6b. (4-(1H-imidazole-1-carbonyl)piperazin-1-yl)(1-(3-(trifluoromethyl)phenyl)-1H-indol-3-yl)methanone. Yield 87%. ^{1}H NMR (500 MHz, $CDCl_3$) δ = 7.83 (s, 1H), 7.71 (s, 1H), 7.64 (dd, J = 13.2, 7.7 Hz, 4H), 7.43 (d, J = 8.3 Hz, 1H), 7.24 (t, J = 7.4 Hz, 2H), 7.16 (d, J = 19.2 Hz, 2H), 7.04 (s, 1H), 3.83 – 3.76 (m, 4H), 3.66 – 3.58 (m, 4H); ESI-MS (m/z) calcd. for $C_{24}H_{21}F_3N_5O_2^+$ $[M+H]^+$ 468.16, found 467.79

6c. (4-benzoylpiperazin-1-yl)(1-(3-(trifluoromethyl)phenyl)-1H-indol-3-yl)methanone. Yield 76%. ^{1}H NMR (500 MHz, $CDCl_3$) δ= 7.79 (s, 1H), 7.76-7.67 (m, 5H), 7.62 (d, J = 6.6 Hz, 1H), 7.50 (d, J = 6.8 Hz, 1H), 7.45-7.39 (m, 4H), 7.33 – 7.29 (m, 2H), 3.81 (br s, 8H); ESI-MS (m/z) calcd. for $C_{27}H_{23}F_3N_3O_2^+$ $[M+H]^+$ 478.17, found 477.79 .

7aN-methyl-N-(2-(N-methyl-4-oxo-4H-chromene-3-carboxamido)ethyl)-5-nitro-1-(3-(trifluoromethyl)phenyl)-1H-indole-3-carboxamide. Yield 50%. ^{1}H NMR (500 MHz, $CDCl_3$) δ = 8.97 (s, 1H), 8.18 (dd, J = 15.4, 8.6 Hz, 2H), 8.01 (s, 1H), 7.85 – 7.63 (m, 5H), 7.53 – 7.39 (m, 4H), 3.97 (s, 2H), 3.92 (s, 2H), 3.40 (s, 3H), 3.10 (s, 3H); ESI-MS (m/z) calcd. for $C_{30}H_{24}F_3N_4O_6^+$ $[M+H]^+$ 592.16, found 592.53.

7b. 3-(4-(5-nitro-1-(3-(trifluoromethyl)phenyl)-1H-indole-3-carbonyl)piperazine-1-carbonyl)-4H-chromen-4-one. Yield 41%. ^{1}H NMR (500 MHz, $CDCl_3$) δ = 8.77 (s, 1H), 8.29 – 8.16 (m, 3H), 7.81 – 7.69 (m, 4H), 7.56 – 7.41 (m, 5H), 3.93 (s, 4H), 3.89 (s, 2H), 3.49 (s, 2H) ; ESI-MS (m/z) calcd. for $C_{30}H_{22}F_3N_4O_6^+$ $[M+H]^+$ 591.15, found 590.79.

7c. N-(2-(2-fluoro-N-methylbenzamido)ethyl)-N-methyl-5-nitro-1-(3-(trifluoromethyl)phenyl)-1H-indole-3-carboxamide. Yield 41%. ^{1}H NMR (500 MHz, $CDCl_3$) δ = 8.97 (s, 1H), 8.20 (d, J = 6.9 Hz, 1H), 7.77-7.68 (m, 4H), 7.56 – 7.41 (m, 2H), 7.41 – 7.28 (m, 1H), 7.14 – 7.01 (m, 2H), 6.97 (d, J = 5.4 Hz, 1H), 3.99 (br s, 4H), 3.39 (s, 3H), 3.04 (s, 3H); ESI-MS (m/z) calcd. for $C_{27}H_{23}F_4N_4O_4^+$ $[M+H]^+$ 543.16, found 542.79 .

8c. 3-(4-(5-nitro-1-(3-nitrophenyl)-1H-indole-3-carbonyl) piperazine-1-carbonyl)-4H-chromen-4-one. Yield 66%. ^{1}H NMR (500 MHz, $CDCl_3$) δ= 8.21 (s, 1H), 7.86 – 7.79 (m, 2H), 7.70 (s, 1H), 7.66 (d, J = 11.0 Hz, 2H), 7.31 (dd, J = 20.7, 8.0 Hz, 2H), 7.21 – 7.13 (m, 1H), 7.01 – 6.94 (m, 2H), 6.93 – 6.88 (m, 1H), 6.71 (s, 1H), 3.37 (s, 6H), 2.90 (s, 2H); ESI-MS (m/z) calcd. for $C_{29}H_{22}N_5O_8^+$ $[M+H]^+$ 568.15, found 567.75.

9a. 4-(2-fluorobenzoyl)piperazin-1-yl)(5-nitro-1H-indol-3-yl)methanone. Yield 25%, Purity 87%. ^{1}H NMR (500 MHz, $CDCl_3$) δ = 8.77 (s, 1H), 8.02 (t, J = 6.4 Hz, 1H), 7.70 (s, 1H), 7.58 (s, 2H), 7.53 – 7.33 (m, 4H), 3.95 – 3.64 (m, 8H) ; ESI-MS (m/z) calcd. for $C_{20}H_{18}FN_4O_4^+$ $[M+H]^+$ 397.13, found 397.00.

9b. (5-nitro-1H-indol-3-yl)(4-(thiophene-2-carbonyl) piperazin-1-yl)methanone. Yield 43%. ^{1}H NMR (500 MHz, $CDCl_3$) δ =8.91 (s, 1H), 8.73 (s, 1H), 8.19 (d, J = 8.9 Hz, 1H), 7.69 (s, 1H), 7.49 (s, 2H), 7.34 (s, 1H), 7.07 (d, J = 3.5 Hz, 1H), 3.84 (d, J = 8.8 Hz, 8H) ; ESI-MS (m/z) calcd. for $C_{18}H_{17}N_4O_4S^+$ $[M+H]^+$ 385.10, found 385.00.

11a. N-(3-(4-oxo-4H-chromene-3-carboxamido)propyl)-1-(phenylsulfonyl)-1H-indole-3-carboxamide. Yield 95%. ^{1}H NMR (500 MHz, $CDCl_3$) δ =9.10 (s, 1H), 8.56 (s, 1H), 7.82 – 7.74 (m, 2H), 7.73 – 7.67 (m, 1H), 7.48 – 7.40 (m, 2H), 7.28 (t, J = 8.6 Hz, 1H), 7.16 – 6.98 (m, 4H), 6.96 (t, J = 7.8 Hz, 2H), 6.85 – 6.80 (m, 2H), 6.77 (s, 1H), 3.13 (dd, J = 12.2, 6.3 Hz, 2H), 3.04 (dd, J = 11.9, 6.0 Hz, 2H), 1.41 (dd, J = 11.9, 6.1 Hz, 2H) ; ESI-MS (m/z) calcd. for $C_{28}H_{24}N_3O_6S^+$ $[M+H]^+$ 530,14 , found 529.75.

11b. N-(4-(2-naphthamido)butyl)-1-(phenylsulfonyl)-1H-indole-3-carboxamide. Yield 54%. ^{1}H NMR (500 MHz, $CDCl_3$) δ =7.92 (s, 1H), 7.81 (s, 1H), 7.64 (d, J = 7.7 Hz, 1H), 7.51 – 7.34 (m, 6H), 7.10 – 6.98 (m, 3H), 6.93 – 6.75 (m, 5H), 6.51 (s, 1H), 6.30 (s, 1H), 3.15 – 3.05 (m, 4H), 1.36 – 1.23 (m, 4H); ESI-MS (m/z) calcd. for $C_{30}H_{28}N_3O_4S^+$ $[M+H]^+$ 526.18, found 525.75.

11c. N-(3-benzamidopropyl)-1-(phenylsulfonyl)-1H-indole-3-carboxamide. Yield 85%. ^{1}H NMR (500 MHz, $CDCl_3$) δ= 8.20 (s, 1H), 8.13 (d, J = 7.4 Hz, 1H), 7.98 (d, J = 8.0 Hz, 1H), 7.90 (dd, J = 21.8, 7.4 Hz, 4H), 7.55 (t, J = 7.5 Hz, 1H), 7.50 (t, J=7.6 Hz, 1H),

7.47-7.40 (m, 3H), 7.39 – 7.31 (m, 2H), 7.25 – 7.17 (m, 1H), 3.62 – 3.51 (m, 4H), 1.88 – 1.80 (m, 2H), 1.70 (s, 1H), 1.25 (s, 1H) ; ESI-MS (m/z) calcd. for $C_{25}H_{24}N_3O_4S^+$ $[M+H]^+$ 462.15, found 461.75.

General procedures for the synthesis of the mixed analogs 10a-e:

Compounds **10a-e** bearing both the amine and the amide moieties were synthesized according to method A1 for the formation of the intermediate amines **iii** and method B2 for the amide coupling.

10a. 3-(4-((1-(3-(trifluoromethyl)phenyl)-1H-indol-3-yl) methyl)piperazine-1-carbonyl)-4H-chromen-4-one. Yield 79% ^{1}H NMR (500 MHz, $CDCl_3$) δ =8.22 (d, J = 9.1 Hz, 1H), 8.16 (s, 1H), 7.82 (d, J = 7.8 Hz, 1H), 7.76 (s, 1H), 7.72 – 7.56 (m, 4H), 7.54 – 7.41 (m, 3H), 7.33 – 7.17 (m, 3H), 3.83 (br s, 4H), 3.41 (br s, 2H), 2.65 (d, J = 24.4 Hz, 5H); ESI-MS (m/z) calcd. for $C_{30}H_{25}F_3N_3O_3^+$ $[M+H]^+$ 532.18, found 531.75.

10b. 3-(4-((5-nitro-1-(3-(trifluoromethyl)phenyl)-1H-indol-3-yl)methyl)piperazine-1-carbonyl)-4H-chromen-4-one. Yield 47%. ^{1}H NMR (500 MHz, $CDCl_3$) δ = 8.80 (s, 1H), 8.21 (d, J = 7.9 Hz, 1H), 8.16-8.14 (m, 2H), 7.74-7.70 (m, 5H), 7.49 (d, J = 8.7 Hz, 2H), 7.44 (t, J = 7.5 Hz, 2H), 3.84 (br s, 4H), 3.42 (br s, 2H), 2.65 (br s, 4H); ESI-MS (m/z) calcd. for $C_{30}H_{24}F_3N_4O_5^+$ $[M+H]^+$ 577.17, found 576.78.

10c. naphthalen-2-yl(4-((1-(3-(trifluoromethyl)phenyl)-1H-indol-3-yl)methyl)piperazin-1-yl)methanone. Yield 43%. ^{1}H NMR (500 MHz, $CDCl_3$) δ = 7.91 (s, 1H), 7.88 – 7.80 (m, 4H), 7.76 (s, 1H), 7.70 (d, J = 7.8 Hz, 1H), 7.62 (dd, J = 16.5, 7.7 Hz, 2H), 7.51 (dd, J = 14.6, 8.1 Hz, 4H), 7.32 – 7.19 (m, 3H), 3.88 (br s, 2H), 3.82 (s, 2H), 3.52 (br s, 2H), 2.60 (d, J = 82.7 Hz, 4H); ESI-MS (m/z) calcd. for $C_{31}H_{27}F_3N_3O^+$ $[M+H]^+$ 514.21, found 514.00.

10d. naphthalen-2-yl(4-((5-nitro-1-(3- (trifluoromethyl) phenyl)-1H-indol-3-yl)methyl)piperazin-1-yl)methanone. Yield =63%. ^{1}H NMR (500 MHz, $CDCl_3$) δ = 8.81 (s, 1H), 8.16 (d, J = 10.5 Hz, 1H), 7.95 – 7.78 (m, 4H), 7.73-7.70 (m, 4H), 7.56 – 7.38 (m, 5H), 4.00 – 3.39 (m, 6H), 2.64 (d, J = 116.7 Hz, 4H); ESI-MS (m/z) calcd. for $C_{31}H_{26}F_3N_4O_3^+$ $[M+H]^+$ 559.20, found 559.02.

10e. phenyl(4-((1-(3-(trifluoromethyl)phenyl)-1H-indol-3-yl)methyl)piperazin-1-yl)methanone. Yield =86%. ^{1}H NMR (500 MHz, $CDCl_3$) δ = 7.81 (d, J = 7.7 Hz, 1H), 7.75 (s, 1H), 7.71-7.69(m, 1H), 7.67 – 7.57 (m, 2H), 7.53 (d, J = 8.2 Hz, 1H), 7.40-7.37 (m, 5H), 7.31 – 7.17 (m, 3H), 3.80 (br s, 4H), 3.44 (s, 2H), 2.56 (d, J = 79.9 Hz, 4H); ESI-MS (m/z) calcd. for $C_{27}H_{25}F_3N_3O^+$ $[M+H]^+$ 464.19, found 464.05 .

General reduction procedures for the synthesis of 3c-d, 4e-f and 8a-b:

Method C1. To solution of the nitro-compound **3b** (0.04 mmol) in absolute ethanol (0.5 mL) and EtOAc (0.5 mL) was slowly added 10% palladium on charcoal (20 mg). The reaction mixture was degassed with vacuum and set under argon. Then argon was removed with vacuum and the reaction mixture was hydrogenated at atmospheric pressure at room temperature until the starting material disappeared according to LC-MS analysis. The reaction mixture was shaken with air and filtered through Celite, and evaporated under reduced pressure. The residue was purified by flash chromatography (gradient system: 1-3% MeOH/DCM) to provide the amine compound **3d.**

3d. 3-(4-(1-(3-aminophenyl)-1H-indole-3-carbonyl)piperazine-1-carbonyl)-4H-chromen-4-one. Yield 96%**.** ^{1}H NMR (500 MHz, $CDCl_3$) δ= 8.22 (s, 1H), 7.81 – 7.68 (m, 2H), 7.65 (s, 1H), 7.59 – 7.38 (m, 3H), 7.34 – 7.15 (m, 4H), 6.87 (d, J = 7.6 Hz, 1H), 6.79 (s, 1H), 6.72 (d, J = 7.9 Hz, 1H), 5.33 (s, 2H), 3.90 (s, 4H), 3.85 (s, 2H), 3.44 (s, 2H); ^{13}C NMR (125.5 MHz, $CDCl_3$) δ 174.00, 163.98, 163.23, 162.14, 157.42, 156.18, 148.47, 139.72, 134.59, 134.39, 132.35, 131.26, 128.86, 128.55, 126.40, 126.30, 126.22, 126.07, 124.99, 124.34, 122.45, 122.37, 121.45, 118.43, 118.25, 113.51, 47.60, 42.64; ESI-MS (m/z) calcd. for $C_{29}H_{25}N_4O_4^+$ $[M+H]^+$ 493.19, found 492.75.

Method C2. The nitro-compound **3a, 4c** or **4d** respectively (0.03 mmol) and Tin(II) chloride dehydrate $SnCl_2{\cdot}2H_2O$ 1M in DMF (1ml) were mixed and stirred at room temperature for 24h. At that time Tin(II) chloride dehydrate $SnCl_2{\cdot}2H_2O$ 1M in DMF (1 mL) was additionally added and the reaction was stirred for another 24h at room temperature. DCM (20 mL) was added and the organic phase was treated with 1N NaOH (1x10 mL), H_2O (2x 10 mL) and brine (1x 10 mL). The organic phase was then dried over Na_2SO_4, filtrated, and the filtrate was concentrated under reduced pressure. The crude residue was purified by flash chromatography (gradient system: 1-10% MeOH/DCM) to provide the amine compounds **3c, 4e** and **4f**.

3c. 1-(3-aminophenyl)-N-methyl-N-(2-(N-methyl-4-oxo-4H-chromene-3-carboxamido)ethyl)-1H-indole-3-carboxamide. Yield 74%. ^{1}H NMR (500 MHz, $CDCl_3$) δ= 8.16 (d, J = 7.1 Hz, 1H), 8.01 – 7.83 (m, 2H), 7.80 – 7.56 (m, 2H), 7.56 – 7.33 (m, 5H), 7.20 (s, 2H), 7.06 (s, 1H), 6.99 (s, 1H), 4.02 – 3.70 (m, 4H), 3.53 (br s, 2H), 3.34 (s, 3H), 3.07 (s, 3H) ; ESI-MS (m/z) calcd. for $C_{29}H_{27}N_4O_4^+$ $[M+H]^+$ 495.20, found 494.95.

4e. 1-(3-aminophenylsulfonyl)-N-methyl-N-(2-(N-methyl-4-oxo-4H-chromene-3-carboxamido)ethyl)-1H-indole-3-carboxamide. Yield 65%**.** ^{1}H NMR (500 MHz, $CDCl_3$) δ= δ 8.30 – 8.14 (m, 1H), 7.94 (s, 2H), 7.76 – 7.64 (m, 2H), 7.58 – 7.49 (m, 1H), 7.43 (d, J = 8.8 Hz, 2H), 7.35 (d, J = 7.6 Hz, 3H), 7.13 (s, 1H), 6.97 (d, J = 8.3 Hz, 1H), 6.68 (s, 1H), 4.31 (br s, 2H), 3.92 (br s, 4H), 3.30 (s, 3H), 3.05 (s, 3H); ESI-MS (m/z) calcd. for $C_{29}H_{27}N_4O_6S^+$ $[M+H]^+$ 559.16, found 558.65.

4f. 3-(4-(1-(3-aminophenylsulfonyl)-1H-indole-3-carbonyl) piperazine-1-carbonyl)-4H-chromen-4-one. Yield 76%. ^{1}H NMR (500 MHz, $CDCl_3$) δ = 7.71 (s, 1H), 7.44 (d, J = 8.1 Hz, 1H), 7.23 – 7.17 (m, 1H), 7.12 (d, J = 4.8 Hz, 1H), 7.03 – 6.92 (m, 3H), 6.84 (t, J = 7.7 Hz, 1H), 6.79 (d, J = 7.4 Hz, 1H), 6.74 (s, 2H), 6.68 (t, J = 7.9 Hz, 1H), 6.60 (s, 1H), 6.27 (d, J = 7.9 Hz, 1H), 3.42 (s, 2H), 3.31 (s, 6H), 2.88 (s, 2H) ; ESI-MS (m/z) calcd. for $C_{29}H_{25}N_4O_6S^+$ $[M+H]^+$ 557.15, found 556.85.

Method C3. To solution of the nitro-compound **8c** (1 mmol) in absolute ethanol (3 mL) and EtOAc (3 mL) was added PtO_2 (15 mg). The reaction mixture was degassed with vacuum and set under argon. Then argon was removed with vacuum and the reaction mixture was hydrogenated at atmospheric pressure at room temperature until the starting material disappeared according to LC-MS analysis. The reaction mixture was shaken with air and filtered through Celite, and evaporated under reduced pressure. The crude residue was purified by flash chromatography (gradient system: 1-10% MeOH/DCM) to provide the target amine compound **8a** and **8b** as a side product.

8a. 3-(4-(5-amino-1-(3-aminophenyl)-1H-indole-3-carbonyl) piperazine-1-carbonyl)-4H-chromen-4-one. Yield 39%. ^{1}H NMR (500 MHz, $CDCl_3$) δ = 8.23 (d, J = 10.2 Hz, 2H), 7.73 (t, J = 10.0 Hz, 1H), 7.57 – 7.49 (m, 2H), 7.49 – 7.43 (m, 1H), 7.36 (d, J = 8.7 Hz, 1H), 7.04 (s, 1H), 6.97 (d, J = 9.0 Hz, 1H), 6.84 (d, J = 9.4 Hz, 1H), 6.75 (s, 1H), 6.72 – 6.63 (m, 2H), 3.89 (s, 4H), 3.85 (s, 2H), 3.64 (s, 2H), 3.42 (s, 2H); ESI-MS (m/z) calcd. for $C_{29}H_{26}N_5O_4^+$ $[M+H]^+$ 508.20, found 507.89.

8b. 3-(4-(5-amino-1-(3-aminophenyl)-1H-indole-3-carbonyl) piperazine-1-carbonyl)chroman-4-one. Yield 31%. ^{1}H NMR (500 MHz, $CDCl_3$) δ= 7.89 (d, J = 8.0 Hz, 1H), 7.54-7.51(m, 2H), 7.36 (d, J = 8.6 Hz, 1H), 7.09-7.01 (m, 4H), 6.84 (d, J = 7.0 Hz, 2H), 6.76 (s, 2H), 6.69-6.65 (m, 3H), 4.21 – 3.99 (m, 6H), 3.86 (s, 2H), 3.65 (br s, 2H), 3.41 (br s, 2H); ESI-MS (m/z) calcd. for $C_{29}H_{28}N_5O_4^+$ $[M+H]^+$ 510.21, found 509.85.

Binding affinity and toxicity assay

Expression and purification of TNF

The extracellular domain of TNF was expressed in BL21(DE3) pLysS strain of *E. coli* as a GST-fusion protein as previously described.[37] GST-TNF was purified as previously described [37] while separation of TNF from its GST fusion partner was accomplished by proteolytic cleavage with the type-14 human rhinovirus 3C protease (America Pharmacia Biotech). The concentration of protein in the samples was determined by the Bradford method[38] using bovine albumin as standard.

Fluorescence binding assay and determination of dissociation constant (K_d)

Fluorescence intensity was measured with a Hitachi F-2500 fluorescence spectrophotometer in 1.0 x 4.5 cm quartz cuvettes at 25 ^{o}C as previously described.[26] A detailed analysis of the development of the fluorescence ligand-binding assay is given in ref.[26] Differences in fluorescence intensity at 302 nm between the complex (TNF/ligand) and free protein (excitation at 274 nm) were analyzed as previously described[26] in order to determine the dissociation constant (K_d) of TNF with various ligands. Experiments were performed in 10 mM citrate- phosphate (pH 6.5) containing either 5% DMSO or 5% PEG3350. The slits were set at 5 and 20 nm in the excitation and emission respectively. In order to determine dilution effect of TNF (due to ligand addition) and any fluorescence effect by unbound ligand, a blank sample containing Tyr with the same fluorescence signal, was titrated with sequential ligand additions.[26] The sample absorbance was kept below 0.1 to minimize the inner filter effect. Data were analyzed using Prism V.5 (GraphPadSoftware, San Diego, CA).

TNF-induced death assay in L929 cells

L929 cells were seeded onto a 96-well plate (3×104 cells/well). On the following day, cells were treated with 0.25 ng/mL human TNF (PeproTech, NJ) and 2 mg/mL actinomycin D (Sigma–Aldrich, MO). To test inhibition by synthesized compounds, TNF was pre-incubated for 30 min at room temperature with the compounds prior to addition to cells. An actinomycin D treated-only control was included to measure background death. After 18–24 h, dead cells were removed by washing with PBS. The remaining live cells were fixed with methanol, stained with crystal violet and quantified spectrophotometrically at 570nm after solubilization of the stain using acetic acid. Cytotoxicity is expressed relative to the background death control as well as to the compounds' toxicity. All experiments were performed in triplicate.

TNF/TNF-R1 ELISA assay

Ninety-six-well plates were coated with 0.1mg/mL recombinant soluble human TNR-R1 (PeproTech) in PBS overnight at 4°C. Following four washes with PBS containing 0.05% Tween-20,blocking was carried out using 1% BSA in PBS. 0.025mg/mL recombinant human TNF (PeproTech) in PBS was added and the plates were incubated for 1 h at room temperature. After another round of washes, plates were incubated with a 1:5000 dilution of a rabbit anti-human-TNF antibody (provided by Prof. W. A. Buurman, University of Maastricht) for 1 h at room temperature. Following another round of washes, plates were incubated with a 1:5000 dilution of an anti-rabbit secondary antibody conjugated with HRP (Vector Laboratories, CA) for 1 h at room temperature. After a final round of washes, the signal was developed using the TMB Substrate Kit (Thermo Scientific, IL) and measured spectrophotometrically at 450 nm. All experiments were performed in triplicate.

Molecular Docking

The crystallographic structure of TNF dimer was retrieved from the Protein Data Bank (accession code 2AZ5). The protein atoms comprising chains A and B were extracted from the PDB file and were used without any further modification for the docking calculations. The initial conformations of the designed scaffolds were generated from SMILES representations using the program Omega v2.3 (OpenEye Scientific Software, Santa Fe, NM. http://www.eyesopen.com) with default parameters.[39] For protein and ligands, only polar hydrogen atoms were added and Gasteiger charges were applied using AutoDockTools v1.5.6. The search space was defined by a grid box centered on the ligand and comprised of 55 × 55 × 41 grid points of 0.375 Å spacing. For each complex, 100 docking rounds were calculated with AutoDock v4.2.3 using the Lamarckian genetic algorithm with the default parameters from AutoDock 3.[40, 41] The maximum number of energy evaluations was set to 10 million and the results were clustered using a tolerance of 2.0 Å. Visual inspection of the resulting complexes and rendering of figures were carried out using VMD v1.9.1.[42]

Acknowledgements

This work was funded by the project TheRAlead (09SYN-21-784) co-financed by the European Union (European Regional Development Fund – ERDF) and Greek national funds through the Operational Program "Competitiveness & Entrepreneurship", NSRF 2007–2013 in the context of GSRT-National action "Cooperation".

Notes and references

[a] Department of Biochemistry Veterinary School, University of Thessaly, Trikalon 224, Karditsa 43100, Greece
[b.] Institute for Research and Technology of Thessaly (I.RE.TE.TH.), The Centre for Research & Technology Hellas (CE.R.TH.), Dimitriados 95 & Paulou Mela, Volos 38333, Greece
[c] Laboratory of General Chemistry, Department of Science, Agricultural University of Athens, Iera Odos 75, Athens 11855, Greece
[d.] Laboratory of Genetics, Department of Biotechnology, Agricultural University of Athens, Iera Odos 75, Athens 11855, Greece
[e.] Biomedical Sciences Research Center "Alexander Fleming", Vari, Greece
[f] pro-ACTINA S.A., Archimidous Str. 59, P.O.Box 205, Koropi, Athens 19400, Greece.

[*]Corresponding author: G.A Kontopidis,
Laboratory of Biochemistry, Veterinary School, University of Thessaly, Trikalon 224, Karditsa 43100, Greece
Tel: +30 24410 66081; Fax: +30 24410 66041
e-mail: gkontopidis@vet.uth.gr

Electronic Supplementary Information (ESI) available: See DOI: 10.1039/b000000x/

1. I. B. McInnes and G. Schett, *New Engl. J. Med.*, 2011, **365**, 2205-2219.
2. H. Maradit-Kremers, P. J. Nicola, C. S. Crowson, K. V. Ballman and S. E. Gabriel, *Arthritis Rheum.*, 2005, **52**, 722-732.
3. R. Atreya, J. Mudter, S. Finotto, J. Mullberg, T. Jostock, S. Wirtz, M. Schutz, B. Bartsch, M. Holtmann, C. Becker, D. Strand, J. Czaja, J. F. Schlaak, H. A. Lehr, F. Autschbach, G. Schurmann, N. Nishimoto, K. Yoshizaki, H. Ito, T. Kishimoto, P. R. Galle, S. Rose-John and M. F. Neurath, *Nat. Med.*, 2000, **6**, 583-588.
4. K. Chatzantoni and A. Mouzaki, *Curr. Top. Med. Chem.*, 2006, **6**, 1707-1714.
5. M. A. Palladino, F. R. Bahjat, E. A. Theodorakis and L. L. Moldawer, *Nat. Rev. Drug Discov.*, 2003, **2**, 736-746.
6. J. Stanczyk, C. Ospelt and S. Gay, *Curr. Opin. Rheumatol.*, 2008, **20**, 257-262.
7. Q. Shen, J. Chen, Q. Wang, X. Deng, Y. Liu and L. Lai, *Eur. J. Med. Chem.*, 2014, **85**, 119-126.
8. M. R. Lee and C. Dominguez, *Curr. Med .Chem.*, 2005, **12**, 2979-2994.
9. H. S. Rasmussen and P. P. McCann, *Pharmacol. Ther.*, 1997, **75**, 69-75.
10. S. Haraguchi, N. K. Day, W. Kamchaisatian, M. Beigier-Pompadre, S. Stenger, N. Tangsinmankong, J. W. Sleasman, S. V. Pizzo and G. J. Cianciolo, *AIDS Res. Ther.*, 2006, **3**, 8.
11. J. R. Burke, M. A. Pattoli, K. R. Gregor, P. J. Brassil, J. F. MacMaster, K. W. McIntyre, X. Yang, V. S. Iotzova, W. Clarke, J. Strnad, Y. Qiu and F. C. Zusi, *J. Biol. Chem.*, 2003, **278**, 1450-1456.
12. C. H. Leung, S. P. Grill, W. Lam, W. Gao, H. D. Sun and Y. C. Cheng, *Mol. Pharmacol.*, 2006, **70**, 1946-1955.
13. B. P. Bandgar, S. A. Patil, B. L. Korbad, S. H. Nile and C. N. Khobragade, *Eur. J. Med. Chem.*, 2010, **45**, 2629-2633.
14. J. Wu, J. Li, Y. Cai, Y. Pan, F. Ye, Y. Zhang, Y. Zhao, S. Yang, X. Li and G. Liang, *J. Med. Chem.*, 2011, **54**, 8110-8123.
15. J. M. Davis and J. Colangelo, *Future Med. Chem.*, 2013, **5**, 69-79.
16. F. Mancini, C. M. Toro, M. Mabilia, M. Giannangeli, M. Pinza and C. Milanese, *Biochem. Pharmacol.*, 1999, **58**, 851-859.
17. R. P. McGeary, A. J. Bennett, Q. B. Tran, K. L. Cosgrove and B. P. Ross, *Mini Rev. Med. Chem.*, 2008, **8**, 1384-1394.
18. M. M. He, A. S. Smith, J. D. Oslob, W. M. Flanagan, A. C. Braisted, A. Whitty, M. T. Cancilla, J. Wang, A. A. Lugovskoy, J. C. Yoburn, A. D. Fung, G. Farrington, J. K. Eldredge, E. S. Day, L. A. Cruz, T. G. Cachero, S. K. Miller, J. E. Friedman, I. C. Choong and B. C. Cunningham, *Science*, 2005, **310**, 1022-1025.
19. H. Sun and G. S. Yost, *Chem. Res. Toxicol.*, 2008, **21**, 374-385.
20. D. S. Chan, H. M. Lee, F. Yang, C. M. Che, C. C. Wong, R. Abagyan, C. H. Leung and D. L. Ma, *Angew. Chem. Int. Ed. Engl.*, 2010, **49**, 2860-2864.
21. D.-L. Ma, D. S.-H. Chana and C. H. Leung, *Chem. Sci.*, 2011, **2**, 1656-1665.
22. K. S. Kumar, P. M. Kumar, K. A. Kumar, M. Sreenivasulu, A. A. Jafar, D. Rambabu, G. R. Krishna, C. M. Reddy, R. Kapavarapu, K. Shivakumar, K. K. Priya, K. V. Parsa and M. Pal, *Chem. Commun. (Camb)*, 2011, **47**, 5010-5012.
23. C. H. Leung, H. J. Zhong, H. Yang, Z. Cheng, D. S. Chan, V. P. Ma, R. Abagyan, C. Y. Wong and D. L. Ma, *Angew. Chem. Int. Ed. Engl.*, 2012, **51**, 9010-9014.
24. C. H. Leung, D. S. H. Chan, M. H. T. Kwan, Z. Cheng, C. Y. Wong, G. Y. Zhu, W. F. Fong and D. L. Ma, *Chemmedchem*, 2011, **6**, 765-768.
25. P. Alexiou, A. Papakyriakou, E. Ntougkos, C. P. Papaneophytou, F. Liepouri, A. Mettou, I. Katsoulis, A. Maranti, K. Tsiliouka, A. Strongilos, S. Chaitidou, E. Douni, G. Kontopidis, G. Kollias, E. Couladouros and E. Eliopoulos, *Archiv der Pharmazie*, 2014, **347**, 1-8.
26. C. P. Papaneophytou, A. K. Mettou, V. Rinotas, E. Douni and G. A. Kontopidis, *Med. Chem. Lett.*, 2013, **4**, 137-141.
27. B. B. Aggarwal and W. J. Kohr, *Methods enzymol*, 1985, **116**, 448-456.
28. G. Chen and D. V. Goeddel, *Science*, 2002, **296**, 1634-1635.
29. A. F. Abdel-Magid, K. G. Carson, B. D. Harris, C. A. Maryanoff and R. D. Shah, *J. Org. Chem.*, 1996, **61**, 3849-3862.
30. J. W. Coe, M. G. Vetelino and M. J. Bradlee, *Tetrahedron Lett.*, 1996, **37**, 6045-6048.
31. G. C. Look, M. M. Murphy, D. A. Campbell and M. A. Gallop, *Tetrahedron Lett.*, 1995, **36**, 2937–2940.
32. J. Matthews and R. A. Rivero, *J. Org. Chem.*, 1997, **62**, 6090-6092.
33. E. K. Woodman, J. G. K. Chaffey, P. A. Hopes, D. R. J. Hose and J. P. Gilday, *Org. Process Res. Dev.*, 2008, **13**, 106-113.
34. C. A. G. N. Montalbetti and V. Falque, *Tetrahedron*, 2005, **61**, 10827-10852.
35. J. J. Mason, J. Bergman and T. Janosik, *J. Nat. Prod.*, 2008, **71**, 1447-1450.
36. G. P. Wei and G. B. Phillips, *Tetrahedron Lett.*, 1998, **39**, 179-182.
37. C. P. Papaneophytou and G. A. Kontopidis, *Protein Expr. Purif.*, 2012, **86**, 35-44.
38. M. M. Bradford, *Anal. Biochem.*, 1976, **72**, 248-254.
39. P. C. D. Hawkins, A. G. Skillman, G. L. Warren, B. A. Ellingson and M. T. Stahl, *J .Chem. Inf. Model.*, 2010, **50**, 572-584.
40. G. M. Morris, H. Ruth, W. Lindstrom, M. F. Sanner, R. K. Belew, D. S. Goodsell and A. J. Olson, *J. Comput. Chem.*, 2009, **30**, 2785-2791.
41. G. M. Morris, D. S. Goodsell, R. S. Halliday, R. Huey, W. E. Hart, R. K. Belew and A. J. Olson, *J. Comput. Chem.*, 1998, **19**, 1639-1662.
42. W. Humphrey, A. Dalke and K. Schulten, *J. Mol. Graph. Model.*, 1996, **14**, 33-38.